Application of the atmospheric Lagrangian particle dispersion model MLDP0 to the 2008 eruptions of Okmok and Kasatochi volcanoes

Réal D'Amours,[1] Alain Malo,[1] René Servranckx,[1] Dov Bensimon,[1] Serge Trudel,[1] and Jean-Philippe Gauthier-Bilodeau[1]

Received 25 November 2009; revised 21 May 2010; accepted 2 June 2010; published 7 October 2010.

[1] The atmospheric transport and dispersion model Modèle Lagrangien de Dispersion de Particules d'ordre zéro (MLDP0) has been in use at the Canadian Meteorological Centre (CMC) for several years. The model is employed to support environmental emergency response activities, in the context of CMC's national and international mandates. MLDP0 is a Lagrangian model in which diffusion is modeled according to a random displacement equation (RDE). MLDP0 is an off-line model and is driven with meteorological fields from CMC's Numerical Weather Analysis and Prediction (NWP) system. MLDP0 can be executed in forward and inverse modes. During the summer of 2008, the important eruptions at Okmok and Kasatochi, in the Aleutians, were cause of considerable concern to aviation, and the model was used extensively to support the Montreal Volcanic Ash Advisory Centre (VAAC). Qualitative comparisons of satellite imagery and MLDP0 outputs show that the model accurately simulated the behavior of volcanic plumes. Inverse simulations based on SO_2 observations of the Okmok plume, at the Washington State University campus in Pullman, Washington, yield emission estimates that agree well with those derived from AURA/OMI. Forward simulations using AURA/OMI SO_2 emission estimates for the Kasatochi eruption of 7 August also compare quite well quantitatively with observations from Environment Canada's Brewer spectrophotometers in Toronto, as well as with concentration maps reconstructed from AURA/OMI scans.

Citation: D'Amours, R., A. Malo, R. Servranckx, D. Bensimon, S. Trudel, and J.-P. Gauthier-Bilodeau (2010), Application of the atmospheric Lagrangian particle dispersion model MLDP0 to the 2008 eruptions of Okmok and Kasatochi volcanoes, *J. Geophys. Res.*, *115*, D00L11, doi:10.1029/2009JD013602.

1. Introduction

[2] The atmospheric transport and dispersion model Modèle Lagrangien de Dispersion de Particules d'ordre zéro (MLDP0) has been in use at the Canadian Meteorological Centre (CMC) for several years for Environmental Emergency Response. The model is also employed to simulate the release of volcanic ash to support the operations of the Montreal Volcanic Ash Advisory Centre (VAAC). During the eruptions of the Okmok and Kasatochi volcanoes in the summer of 2008, MLDP0 was used extensively and provided useful information to both scientific and aviation communities.

[3] This paper briefly describes MLDP0 and simulations of plumes generated by the eruptions of Okmok in July 2008 and Kasatochi in August 2008 are presented and discussed. We show examples from the real-time simulations, executed when limited information about the eruption was available. We then examine results from a quantitative analysis of SO_2 transport based on forward and inverse modeling, together with data available from AURA/OMI satellite remote sensing, as well as some ground-based observations (Washington State University, Pullman, Washington, USA and Environment Canada, Toronto, Ontario, Canada).

2. A Brief Description of MLDP0

2.1. MLDP0: A Lagrangian Model

[4] In the context of Lagrangian modeling, dispersion in the atmosphere is estimated by calculating the trajectories of a very large number of individual air particles (or fluid elements) in order to adequately represent the dispersing plume. These particles are assumed to conserve their identity during their travel and can transport some amount of material which, depending on its nature, may be subject to various physical processes like dry deposition, wet scavenging, and radioactive decay.

[5] For efficiency reasons, especially when considering transport on a regional or larger scale, a dispersion model is usually an off-line model which uses meteorological fields provided by a NWP system. MLDP0 is driven by the CMC's Global Environmental Multiscale (GEM) NWP

[1]Canadian Meteorological Centre, Dorval, Québec, Canada.

0148-0227/10/2009JD013602

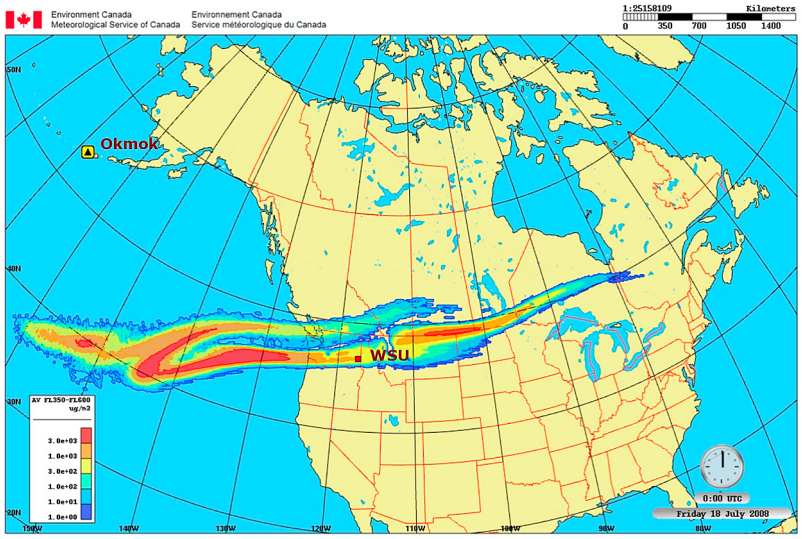

Figure 1. An example of real time product: MLDP0 estimation of the "fine ash" (see text) concentration, in μg m^{-3}, within the layer FL350–FL600 (the layer between aviation flight levels 35,000 feet and 60,000 feet above sea level), valid 18 July 0000 UTC. The red square indicates the location of the Washington State University (WSU) MFDOAS spectrometer.

system (http://www.msc-smc.ec.gc.ca/cmc/op_systems/index_e.html). The meteorological fields (3-D winds, air temperature, relative humidity, to name a few) are available only at certain time intervals and only at a limited number of discrete points in space (3-D grids). Furthermore, dispersion models will very often be used "after the fact," to estimate the behavior the plumes in diagnostic mode. In these cases, dispersion simulations will be based on analyzed meteorological fields, which are generally available at 6-h time intervals. Therefore many scales of motion are not resolved. This is especially true of the turbulent components of the wind which are mostly responsible for the mixing of air parcels. The information provided by the NWP systems can be used to estimate at least some of the statistical properties of atmospheric turbulence. Vigorous turbulent mixing occurs mostly in the atmospheric boundary layer (ABL) near the ground surface, and dispersion models focus on that part of the atmosphere. Details can be found in R. D'Amours and A. Malo (A zeroth order Lagrangian dispersion model MLDP0, internal report, Canadian Meteorological Centre, 2004).

[6] There is no general parameterization for turbulence in the free troposphere (FT), which locally can be generated by gravity waves or deep convection. Very often substances injected above the ABL travel in fairly well maintained streams for several days [*Colette et al.*, 2008; *Gerasopoulos et al.*, 2006]. In MLDP0, the vertical diffusion coefficient falls to a very low threshold value above the boundary layer, and essentially dispersion results from stretching and deformation induced by the horizontal winds, as well as vertical transport associated with fronts and large-scale pressure systems.

[7] An inverse version of MLDP0 has been developed and is used to support the operations of the Comprehensive Nuclear Test Ban Treaty (CTBT) Organization [*World Meteorological Organization* (*WMO*), 2007] (Appendix I-6, Regional and global arrangements for atmospheric backtracking and Appendix II-9, Products provided by RSMCs with activity specialization in atmospheric transport modeling – backtracking for CTBT verification support). The results of inverse simulations are often referred as Source Receptor Sensitivity (SRS) coefficients [*Wotawa et al.*, 2003]. Simply put, the SRS coefficients (usually in units of m^{-3}) are a measure of the amount of air transported from a given region of the atmosphere (a possible source location) into the sampler where the concentrations are measured.

2.2. Operational Applications of MLDP0

[8] MLDP0 is designed for medium and long-range dispersion and has been in use for several years at CMC to support various types of activities associated to national and international mandates. CMC holds the following international designations: (1) VAAC Montreal through the International Civil Aviation Organization (ICAO) and (2) Regional Specialized Meteorological Centre (RSMC) Montreal through the World Meteorological Organization (WMO) and International Atomic Energy Agency (IAEA) [*WMO*, 2007]. The model is used by VAAC Montreal and RSMC Montreal operational staff to predict and track volcanic ash/gas as well as radioactive material released by nuclear accidents. The model is an important element in CMC's contribution to Canada's Federal Nuclear Emergency Plan (FNEP). MLDP0 is also regularly used in various environmental emergencies such as smoke from forest fires, dust storms, toxic spills in the atmosphere and chemical fires.

[9] As reported by R. D'Amours and A. Malo (A zeroth order Lagrangian dispersion model MLDP0, internal report, Canadian Meteorological Centre, 2004) the model was validated with data from ETEX [*van Dop et al.*, 1998] and data from the accidental radioactive release in Algeciras, Spain, in May of 1998. The model is used regularly to track plumes of radio-xenon observed in the Ottawa Valley; some

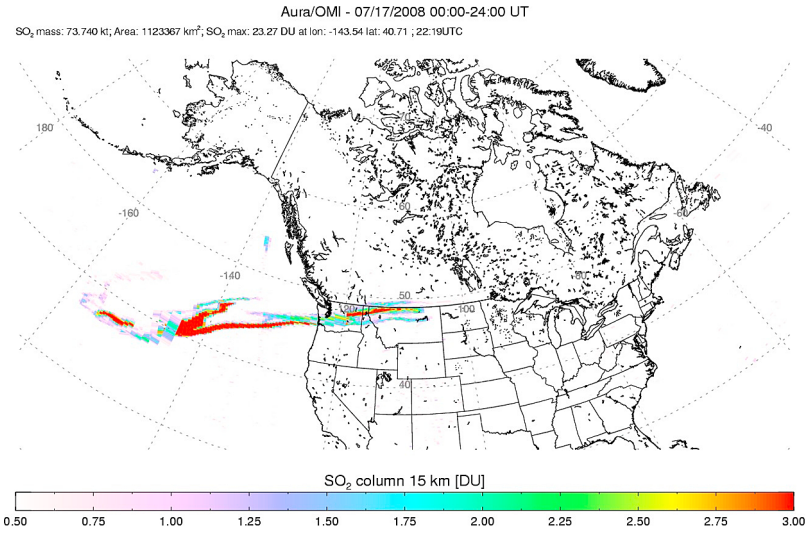

Figure 2. Total column SO_2 concentration derived from AURA/OMI scans, for 17 July 2008.

results are discussed in the work of *Stocki et al.* [2008]. In support of Nuclear Test Ban Treaty verification, MLDP0 was used in the context of a global backward ensemble dispersion modeling study [*Becker et al.*, 2007]. More recently, two independent studies were conducted using MLDP0 to test source parameters for volcanic ash [*Webley et al.*, 2009] and to investigate meteorological influences on particle fallout sedimentation [*Durant and Rose*, 2009] for the August and September 1992 eruptions of Mount Spurr, Alaska.

2.3. Volcanic Ash Modeling

[10] Volcanic eruptions can behave in many ways [*Sparks et al.*, 1997]. Often, the height of an eruption column is a good indicator of the intensity of the ash emission. For a maintained eruption, *Sparks et al.* [1997] have determined an empirical power law for the plume height in terms of the rate of discharge of erupted material. *Mastin et al.* [2009] obtained a result which is not significantly different from the best-fit equation of *Sparks et al.* [1997]. Because the initial plume height, the time of the eruption, and perhaps a duration estimate are the few parameters that could be reported in real time, *Sparks et al.* [1997] formula is very useful for an initial evaluation of the ash emission. However, most of the mass ejected in the atmosphere is deposited very close to the volcano. Less than 10% of the total released mass is transported at distances greater than 10 km [*Sparks et al.*, 1997], and only this fraction is of interest to long-range transport.

[11] Gravitational settling can be an important factor, especially in the early stages of the plume dispersion. In MLDP0 the settling velocity is simply modeled in terms of a

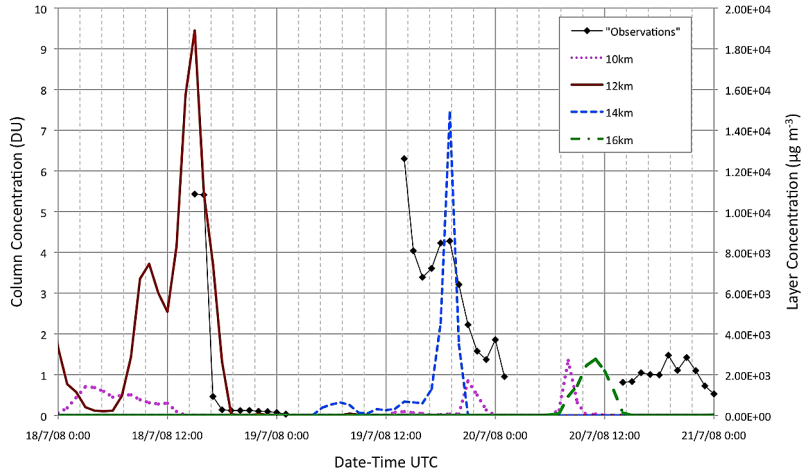

Figure 3. Time series of total column SO_2 concentration (DU) observations at the Washington State University Pullman Campus, left-hand side axis, and model average layer concentrations (μg m^{-3}), right-hand side axis, resulting from a forward simulation, using a uniformly distributed emission in the vertical from the surface to 15 km. The observations were averaged over 1 h, to correspond to the model averaging period. Comparison of timings and relative intensities can be made in order to estimate at which level the observed SO_2, should be found.

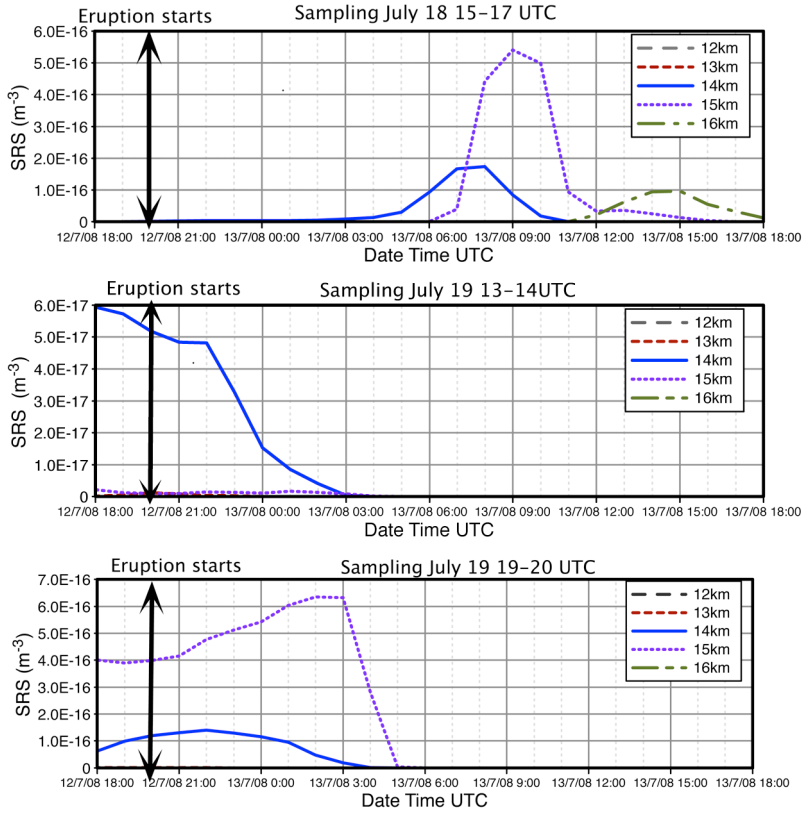

Figure 4. Source-receptor-sensitivity (SRS) coefficient of the 15 km column above the Washington State University Pullman Campus, to different levels above the Okmok Volcano. The SRS is a measure of the amount of air coming from the volcano location, during a given period of time, the sampling period. Values are shown for three sampling periods at WSU, when SO_2 measurements are significant, as a function of origin time at Okmok.

terminal velocity according to Stokes' relationship for a spherical particle. Ash particle size distribution varies greatly depending on the eruption. Empirical distributions based on eruptions of the Redoubt volcano, as reported by *U. S. Geological Survey* [1990] and *Durant and Rose* [2009] for eruptions of Crater Peak (Mount Spurr), as well as improved eruption parameters based [*Mastin et al.*, 2009] study can be used in MLDP0. In most cases however, dispersion modeling is used to assess the transport of very fine ash at long distances from the volcano (for aviation interests as an example); in those cases only particles with small diameters are considered. Considering the large uncertainties in the emission parameters, in a real time response, 10% of the emission rate provided by *Sparks et al.* [1997] is normally used as source term for fine ash, for which gravitational settling is not considered.

3. Modeling the Eruptions of the Summer 2008

[12] The Okmok and Kasatochi volcanoes in the Aleutians were very active during the summer 2008 and several eruptions affected or threatened the Canadian airspace. VAAC Montreal issued several volcanic ash advisory messages and charts on the probable evolution of the ash plumes. Dispersion models were used to provide estimates of plumes motion and intensities, based on incomplete source term information. A fair amount of satellite data on

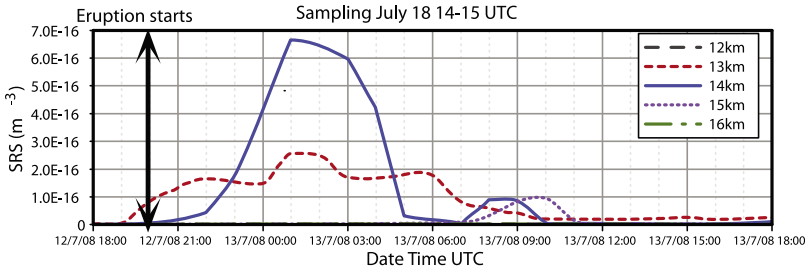

Figure 5. Same as in Figure 4, but for a sampling period just after the first observed SO_2 peak.

Table 1. Maximum Source-Receptor Sensitivity Coefficients for the Washington State University Measurements[a]

Sampling Period for SRS Calculation (UTC)	Maximum SRS at Okmok (no units)	Layer of Maximum SRS (km)	Time of Maximum in Hours From Eruption Start	Peak Observed Concentration (DU)	Estimated Total Emission (g)
18 Jul 1500–1700	5.4E−16	15–16	13	8.7	1.6E+11
18 Jul 1400–1500	6.7E−16	14–15	5	8.7	1.3E+11
19 Jul 1300–1400	2.6E−17	14–15	0	7.4	2.8E+12
19 Jul 1900–2000	6.4E−16	15–16	6	5.8	9.1E+10

[a]Maximum value of the source-receptor sensitivity (SRS) coefficient is used together with the maximum observed total column concentration, during the sampling period used for the inverse simulation.

the plumes, including SO_2 concentrations, became available during and after the eruptions. The satellite images were compared qualitatively with the dispersion model outputs. A few examples are shown and discussed briefly as part of this study. Also total air column SO_2 concentrations are used for quantitative assessments of the model performance and of the capabilities for the estimation of the emission characteristics through inverse modeling. The focus is on the early phases of the eruption episodes, which lasted several weeks in total.

3.1. Okmok Eruption of July 2008

3.1.1. Initial Operational Modeling

[13] Okmok's eruptive episode started with an explosive event occurring suddenly 12 July 1943 UTC, as reported by the Alaska Volcano Observatory (AVO). An ash column rose rapidly to 15 km, well above the tropopause, which is estimated to have been around 11.8 km over the volcano at that time. The initial explosive event lasted several hours; peak seismicity was reached at about 2200 UTC, 12 July, then declined gradually afterward. The eruption continued for over 5 weeks at lower intensities. Early AURA/OMI imagery showed the volcanic plume moving slowly southeastward. Large amounts of SO_2 were injected into the upper atmosphere.

[14] The first operational simulations of the dispersion model MLDP0 were executed on 14 July, with a release scenario based on the initial reported plume height, and using the emission rate derived with the best-fit equation of *Sparks et al.* [1997] to estimate the total amount of ash released in the atmosphere. A continuous constant rate of emission with a duration of 6 h was assumed; this appeared reasonable, in the absence of any other information. Meteorological fields were provided by the CMC GEM Regional NWP system. These simulations indicated that the ash cloud would likely affect Canadian airspace. During the next 10 days, VAAC Montreal continued to track the cloud over Canada and US, in close coordination with VAAC Anchorage and VAAC Washington, using satellite data as well as updated analyzed and forecast meteorological fields for the dispersion modeling. Visual comparisons between the resulting modeled ash plume and the SO_2 concentration fields reconstructed from the AURA/OMI instrument show a fairly good correlation. Figure 1 is an example of guidance provided in real time to aviation meteorologists, and shows a model estimation of the "fine ash" concentration at high levels, 5 days after the start of the eruption, on 18 July 0000 UTC. 10% of the estimated total ash release is considered as fine ash for which gravitational settling is neglected. Figure 2 shows the total column concentration of SO_2, constructed from the AURA/OMI scans on 17 July. The time match of the two images is not exact since the model plume represents a 1-h average for the period ending 18 July, 0000 UTC, and the satellite field is a juxtaposition of the scans from successive orbits. However, the scans over the plume sectors were done just before 18 July, 0000 UTC, so the time correspondence is adequate. The main morphologic features of the plume are well reproduced by the model, even the hook shape over the Pacific. According to the model, this results from a folding of the plume: the leading edge of the plume initially moved southwestward, then curved cyclonically eastward catching up with the trailing edge.

3.1.2. Modeling SO_2 Transport

3.1.2.1. Estimation of the Emission

[15] The measurements of total column SO_2 concentration, resulting from the passage of the Okmok plume above the Multifunction Differential Optical Absorption Spectroscopy (MFDOAS) instrument at Washington State University (WSU), Pullman, Washington, provided time series over 3 days, giving an opportunity for quantitative estimates. Of course these observations give no information on the vertical distribution of the SO_2. In order to estimate the vertical

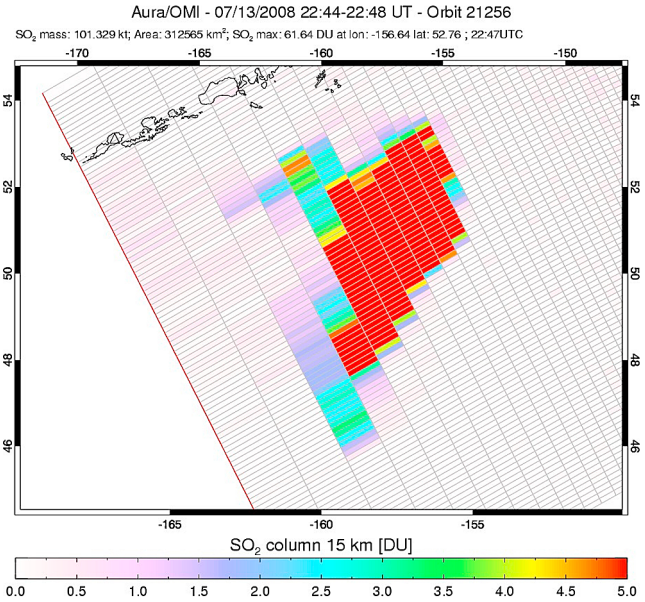

Figure 6. AURA/OMI total SO_2 content (indicated above the map) of the Okmok plume a few hours after the eruption. The shown value of 101.329 kilotons (later revised to 110 kilotons (S. Carn, personal communication, 2009)) compares well with the estimation resulting from inverse modeling (see text).

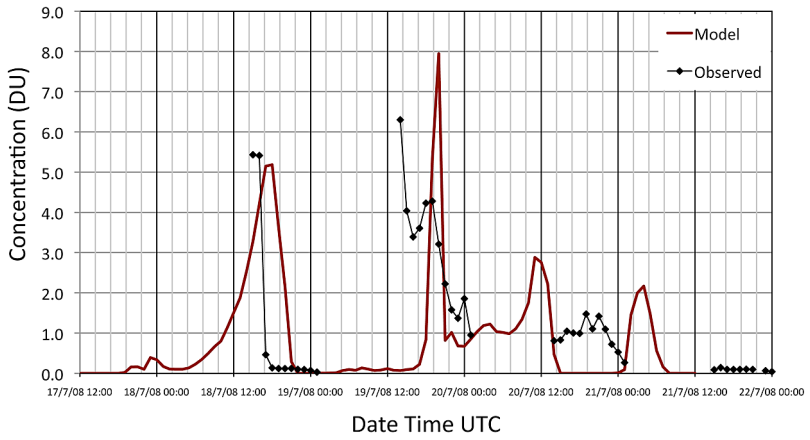

Figure 7. Time series of MLDP0 SO_2 column concentration estimates (DU) resulting from a forward simulation using a 100-kiloton emission, compared with WSU measurements.

distribution of the observed SO_2, an exploratory dispersion simulation was done. The emission was uniformly distributed over a column 15 km high, since at this stage, one cannot make any hypothesis as to which part of the eruption column affected the WSU site. The same amount and duration as the initial runs are used. Also, because the plume was traveling near the edge of the domain of the earlier model simulations, which were based on regional NWP data, in order to avoid possible boundary effects, a hemispheric grid was used, with meteorological data from the CMC GEM global NWP system, at a horizontal resolution of approximately 33 km.

[16] Concentrations were calculated for several 1-km-thick layers, above the location of the MFDOAS instrument in WSU, and can be compared with the measurements in Figure 3. According to the model, the bulk of the observed total concentrations appears to be caused by SO_2 streams traveling in the lower stratosphere; the tropopause was estimated to be between 10 km and 12 km above ground during the period. The measurements from MFDOAS-WSU are available during daytime, 18–20 July. On 18 July, the modeling indicates material from Okmok at levels between 10 km and 14 km and on 19 July, only in the 12 km to 14 km layer. The observations show two peaks on 19 July; the model seems to reproduce only the later one. The model does not show anything on 20 July, however, it indicates the presence of material on 17 July, where there is no data.

[17] This information was then used as a basis for MLDP0 inverse simulations to better characterize the SO_2 discharges from Okmok. It was assumed that the column concentrations over WSU resulted from evenly distributed SO_2 in the layer 12–15 km above ground. Inverse runs were done for observation sampling periods around the three peaks: 18 July 1500–1700 UTC (observation 1), 19 July 1400–1600 UTC (observation 2), and 19 July 1900–2000 UTC (observation 3). Figures 4a, 4b, and 4c show the SRS values, for a period of a few hours after the beginning of the eruption for 1-km-thick layers, starting from 12 km. Essentially, the MFDOAS-WSU location shows sensitivity in the layers 14–15 km and 15–16 km. Interestingly, at the time of observation 3, the MFDOAS-WSU location is more sensitive to Okmok at the beginning of the eruption, while at the time of the earlier observation 1, the location was seeing air which originated from Okmok several hours later; this correlates with the folding process described earlier. The layer of maximum sensitivity is between 14 km and 15 km, for observation 1, and between 15 km and 16 km for observation 3. There is also some sensitivity at these levels for observation 2, but it is an order of magnitude lower. This is consistent with the results of the exploratory forward simulation. However, there appears to be an inconsistency between the forward and inverse simulations for 18 July. The forward simulation, which is based on a 6-h long emission, clearly shows material reaching over the MFDOAS-WSU site on 18 July, during the observation period, while the inverse simulation does not show any significant sensitivity until 10 h after the start of the eruption. This is likely because, for practical reasons, the configurations of the forward and inverse versions of MLDP0 are not exactly the same. Figure 5 shows SRS for the 1-h period before the observation, and there is indeed quite a bit of sensitivity in the first 6 h. This illustrates that the smaller scale features resolved by the measurements must be interpreted with care when compared with larger-scale model results.

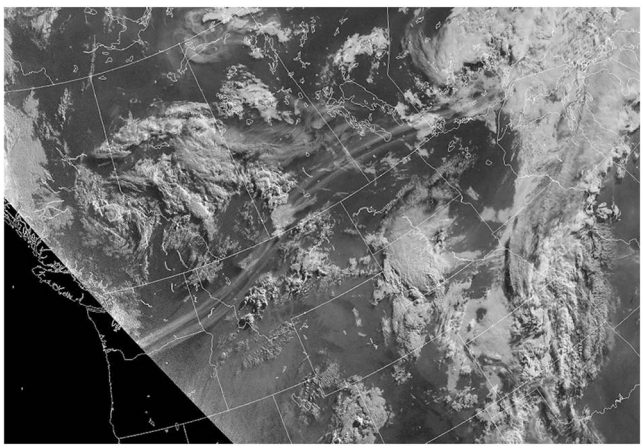

Figure 8. GOES-West image in the visible, valid 18 July 1245 UTC, showing the aerosol plume associated with the SO_2 plume.

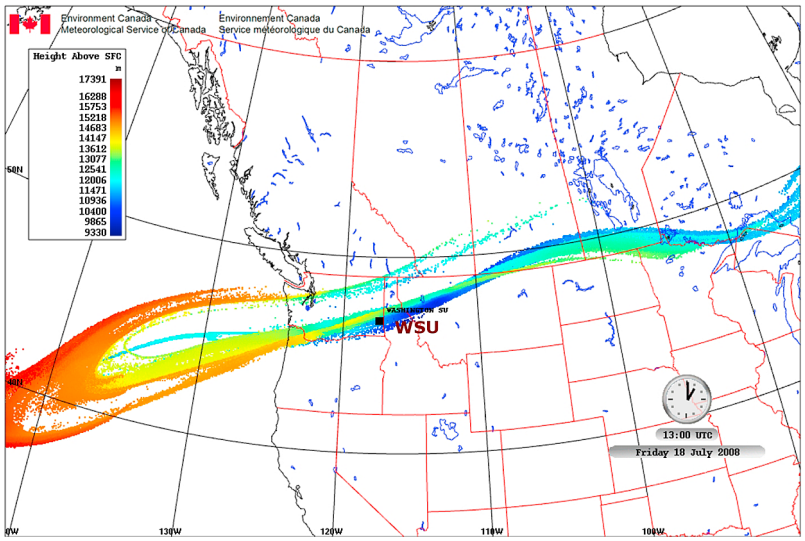

Figure 9. Position of MLDP0 particles, 18 July 1300 UTC. Height above ground in meters is indicated by the color scale. The black square indicates the location of the Washington State University (WSU) MFDOAS spectrometer.

[18] An elaborate reconstruction of the emission profile as done by *Eckhardt et al.* [2008] is beyond the scope of the present study. However, a crude estimation is attempted. In Table 1, the peak concentration measured in the three periods considered is compared to the maximum SRS obtained for that period. The total column concentrations were converted to an average concentration per unit volume in the 3-km-thick layer. The simple arithmetic comparison yields a release of the order of 10^{11} g or 100 kilotons, not taking into account the first peak observed on 19 July, which is not properly captured in the model. This crude estimation is quite consistent with the value of 110 kilotons obtained by

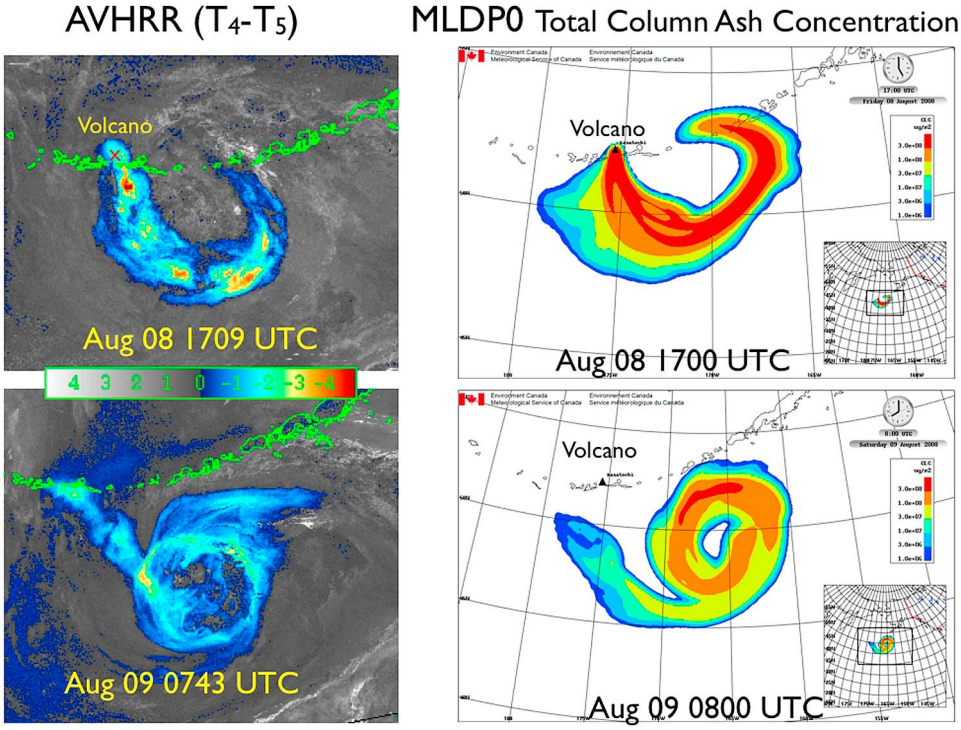

Figure 10. Comparison of Advanced Very High Resolution Radiometer (AVHRR) imagery (NOAA-16 and NOAA-17) showing brightness temperature differences ($T_4 - T_5$) with MLDP0 total column ash concentration, (μg m^{-2}). The plumes are resulting from the Kasatochi eruption. The red cross on the top left indicates the approximate position of the volcano.

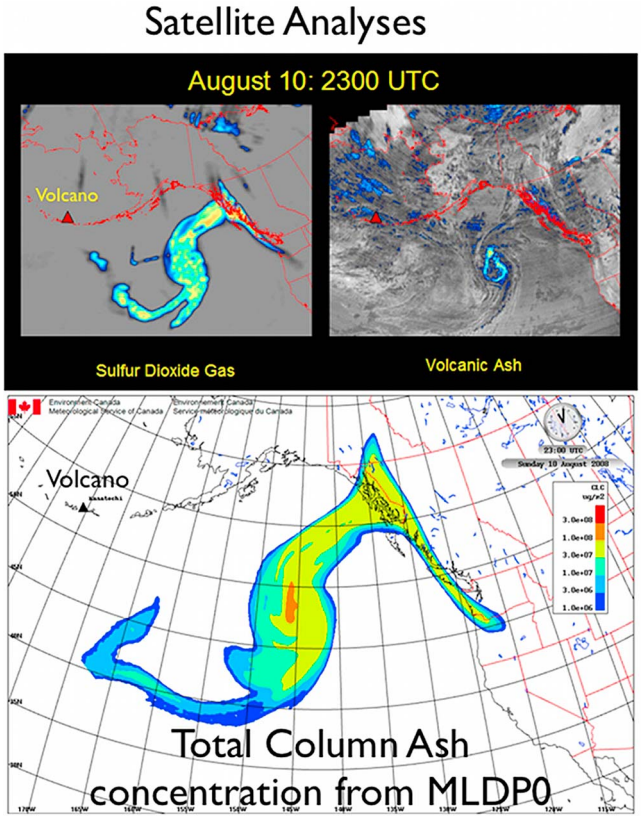

Figure 11. Comparison of AURA/OMI SO_2 gas and AVHRR ($T_4 - T_5$) imagery with MLDP0 total column ash concentration (μg m^{-2}) on 10 August 2300 UTC, for the Kasatochi eruption.

Simon Carn (personal communication, 2009). An initial value of 101.329 kilotons, obtained from the AURA/OMI data, was reported in Figure 6.

3.1.2.2. Validation in Forward Mode

[19] A forward simulation was performed with an emission of 100 kilotons, at a constant rate during 16 hours from the start of the eruption. This revised duration is based on Figure 4a, which indicates that the observed peak on 18 July was sensitive to the volcano between 10 to 16 h after the start of the eruption, as well as on Figure 6, which seems to indicate that significant SO_2 emissions had ceased only a few hours before the satellite scan. The discharge was, somewhat arbitrarily, distributed between 12 km and 16 km as follows: 10% in the layer 12–13 km, 20% between 13 and 14 km, 40% in the layer 14–15 km, and 30% 15–16 km, using the fact that the measuring site was sensitive to those levels only. The resulting total column concentrations at the MFDOAS-WSU location can be compared with the observations in Figure 7. The simulated concentrations are quite in line with the measurements. As expected, the early peak of 19 July is not reproduced. There is less material showing up on 17 July, and during the early hours of 18 July, than in the simulation with the uniform column emission (Figure 3).

[20] Figure 8 shows an early morning visible image from GOES West valid 18 July 1245 UTC, over the northwestern United States and southern Canadian Prairies. Owing to the low Sun angle, the aerosol plume associated with the SO_2 cloud is easily detectable. The elongated and thin structures in the plume are quite remarkable and indicative that it was not subject to much mixing, even after more than 5 days of traveling time. Figure 9 shows the plume formed by the model particles at 1300 UTC on 18 July, just 15 min later than the GOES image. The thin stream-like structure is also evident there. The general position of the main plume is in fairly good agreement with the visible plume. The model shows a double structure as in the satellite image but with more separation. In the model, the northern portion results from a folding of the plume. While there is some evidence of such a process on the AURA/OMI imagery (Figure 2), it is not clear that the double band structure on the visible GOES image (Figure 8) is the result of that process; it would appear more likely that it is related to a fine-scale feature in the southern branch, which is not (and not expected to be) well resolved by the model. It could also be conjectured that the sharp peaks in the observed time series result from denser streams passing overhead as the whole plume meanders eastward. As it was mentioned in section 3.1.2.1, these small scale features could have induced larger-scale responses in the inverse modeling.

3.2. Kasatochi Eruption of August 2008

3.2.1. Initial Operational Modeling

[21] The Kasatochi volcano started to erupt on 7 August, around 2000 UTC, with an explosion that produced an ash and gas plume reaching as high as 14 km. Two other explosions separated by a few hours followed on 8 August 0150 UTC and 8 August 0435 UTC. According to the AVO, the eruption lasted nearly 20 h, with more or less continuous intense gas and ash discharges.

[22] The plume was rapidly caught in a strong cyclonic circulation associated with a well-formed weather system that moved slowly southeastward over the Gulf of Alaska and western Pacific as it was weakening. As a result, the plume was subjected to extensive stretching and deformation but remained very easily detectable on satellite imagery. The persistent volcanic ash clouds caused considerable disruption to airline operations during several days and were closely monitored by the Anchorage, Washington, and Montreal VAACs.

[23] To support Montreal VAAC operations, MLDP0 was executed using a source term based on the best-fit equation of *Sparks et al.* [1997] and an initial plume height of 14 km, with the duration estimated by AVO. The driving meteorological fields were provided by the GEM Regional NWP system. The simulations were quite useful in describing the evolution of the plume and in assessing its arrival over Canadian airspace (Figures 10 and 11). As for the Okmok event, several runs were performed on a daily basis during nearly 2 weeks, utilizing updated analyzed and forecast meteorological data.

3.2.2. Estimating Volcanic Ash Dispersion

[24] Figure 10 shows images derived from the Advanced Very High Resolution Radiometer (AVHRR) sensors on NOAA-16 and NOAA-17 satellites, which can be compared with MLDP0 total column ash concentrations estimates for nearly the same times. The AVHRR imagery is showing brightness temperature differences ($T_4 - T_5$). The negative differences, emphasized on the images, indicate the likely presence of volcanic ash, as described by *Prata* [1989a,

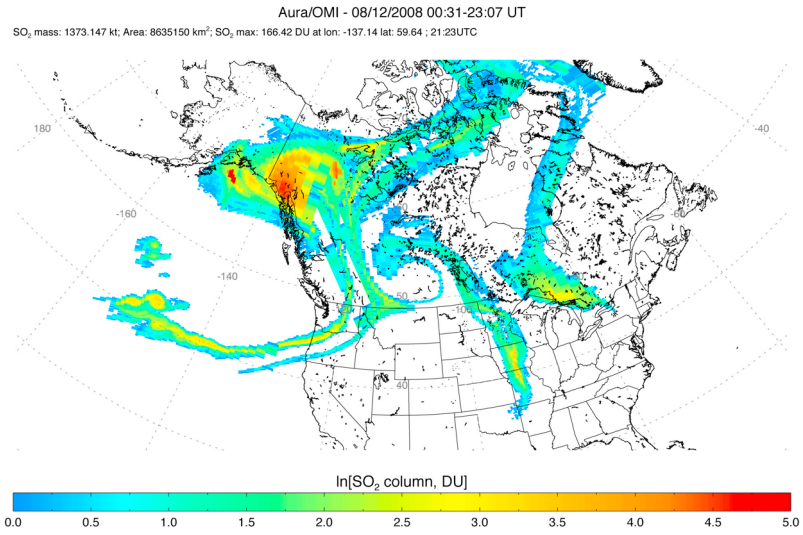

Figure 12. Kasatochi SO_2 plume reconstructed from AURA/OMI scans, for 12 August 2008. Total column concentration (DU) are shown.

1989b]. This technique, also known as the split-window technique, or reverse-absorption technique, takes advantage of the opposite absorption characteristics of water vapor or water/ice clouds and volcanic ash clouds in the infrared channel 4 (10.3–11.3 μm) and channel 5 (11.5–12.5 μm). The satellite images in Figure 10 and Figure 11 were produced by John Bailey (AVO). Both the model and the imagery indicate that the plume became rapidly wound up in the cyclonic flow, drifting southeastward with the low-pressure system. The texture of the plume is patchier on the satellite images. According to the imagery (top left hand side image Figure 10), the volcano is still releasing significant amounts of ash 9 August 1709 UTC, i.e., more than 19 h after the start of eruption, supporting the 20-h long emission scenario.

[25] In Figure 11, the areas of ash estimated by the model are significantly larger than what appears to be detected with the $(T_4 - T_5)$ technique. In fact, the shape of the model ash plume is much more similar to that of the SO_2 plume, also seen in Figure 11. MLDP0 accurately simulates the arrival of material from the eruption on the West Coast. With the information available for this study, the specific reasons for the differences cannot be established. However, the general limitations and uncertainty factors of the split-window technique [*Tupper et al.*, 2004], and of the model simulations [*Servranckx and Chen*, 2004], are known. Certainly, the presence of ash in the plume on the coast should not be discounted.

3.2.3. Modeling SO_2 Transport

[26] The AURA/OMI data show that large quantities of SO_2 dispersed eastward over North America in fairly complex patterns (e.g., Figure 12). The initial MLDP0 simulations had also shown complex dispersion patterns which compare well with the satellite imagery.

[27] The total SO_2 mass estimations derived from the AURA/OMI data are much larger than those for Okmok and

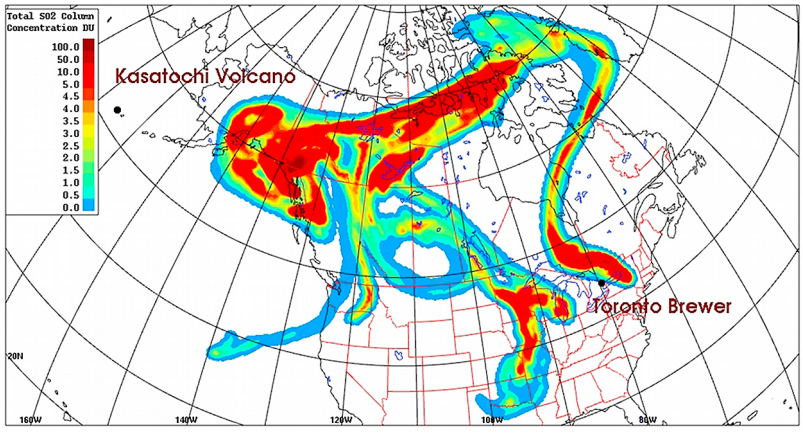

Figure 13. Total SO_2 column concentration (DU) resulting from a MLDP0 forward simulation, using a total emission of 1.3 megaton over 20 hours, starting 7 August 2000 UTC from Kasatochi. The image is valid 12 August 2100 UTC and can be compared with Figure 12. The Toronto location of Environment Canada's Brewer spectrophotometers is indicated on the map.

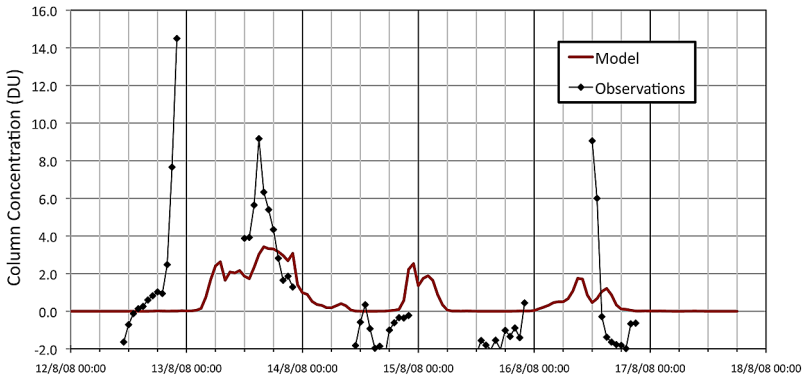

Figure 14. Time series of MLDP0 SO_2 column concentration estimates (DU) in Toronto, compared with the Environment Canada's Brewer spectrophotometer measurements. The observations were averaged over 1 h to correspond with the model estimations.

reach over 1000 kilotons. Because of the good agreement obtained between emission estimates derived from inverse modeling in the case of Okmok, and those derived from AURA/OMI, a forward simulation for SO_2 dispersion was done using a release quantity of 1.3 megaton based on AURA/OMI data (see total mass estimation reported on top of Figure 12). The release was distributed mostly in the high levels, 50% between 10 km and 14 km, at a constant rate for 20 h. For the same reasons as those discussed for the Okmok simulations, the meteorological fields used to drive MLDP0 were provided by the GEM Global NWP system (33 km horizontal resolution).

[28] Total column mass concentrations were calculated and converted to Dobson units (DU). The model results for 12 August 2100 UTC, 5 days after the eruption began, are shown in Figure 13. The patterns are very similar to AURA/OMI SO_2 composite observations (Figure 12). The maximum value shown by the model is 192, compared to 166 for AURA/OMI, and the locations are very close to each other as well. In general, however, the model shows concentrations a few DU higher than observed.

[29] Multiple Brewer Spectrophotometer [*Fioletov et al.*, 1998] instruments at Environment Canada (EC) in Toronto, Canada, detected significant SO_2 total column concentrations during the daytime hours, 12–13 August and again on 16 August; values are below background 14–15 August. These data are presented in Figure 14. On 12 August, the measurements appear to be higher than what could be expected from a quick look at the maps reconstructed from the AURA/OMI orbits. The difference between the AURA/OMI and the ground-based estimates is interesting: it could be due, among other things, to the fact that the map is a reconstruction from discrete orbital scans taken at different times during the day. These orbits do not overlap exactly in time and space, thus perhaps missing some features when the plume is changing rapidly.

[30] The Brewer spectrophotometer measurements can be compared with time series extracted from the modeled plume over the same location in Figure 14. The model values are lower than the measured ones. The model does not pick up the peak of 12 August; however, the model map does show values of the order of those measured from the surface just a bit to the northeast of the observation site. The model also indicates SO_2 passing over the site 13 August, which is detected by the daytime observations, but at a higher level than the modeled one. The model also shows SO_2 traveling over Toronto, on 16 August, nearly 10 days after the start of the eruption, which is confirmed by the observations.

4. Conclusion

[31] The large plumes generated by the eruptions of the summer 2008 at Okmok and Kasatochi, together with the abundance of high-quality satellite imagery provided an exceptional opportunity to illustrate the usefulness of the model in assessing the motion and dispersion of volcanic plumes over medium and large scales.

[32] Ground based observations of column SO_2 concentrations combined with those derived from AURA/OMI allowed for quantitative comparison of model results. These comparisons show that the model can produce realistic estimates of air concentrations at long range in forward mode and realistic estimates of emissions in inverse mode. The SO_2 dispersion patterns observed on the satellite imagery and the model results show that dilution in the upper troposphere and the stratosphere is mostly the result of deformation, shearing, and stretching caused by the winds.

[33] **Acknowledgments.** We wish to thank Simon Carn (Michigan Technological University) and Fred Prata (Norwegian Institute for Air Research) for SO_2 data derived from AURA/OMI, Dave Schneider and John Bailey (Alaska Volcano Observatory) for processed satellite imagery of SO_2 and ($T_4 - T_5$) images, George Mount and Elena Spinei (Washington State University) for total column SO_2 measurements, and Vitali Fioletov and David Tarasick (Environment Canada) for the SO_2 observations derived from the Brewer spectrophotometers.

References

Becker, A., et al. (2007), Global backtracking of anthropogenic radionuclides by means of a receptor oriented ensemble dispersion modelling system in support of nuclear-test-ban treaty verification, *Atmos. Environ.*, *41*(21), 4520–4534, doi:10.1016/j.atmosenv.2006.12.048.

Colette, A., L. Menut, M. Haeffelin, and Y. Morille (2008), Impact of the transport of aerosols from the free troposphere towards the boundary layer on the air quality in the Paris area, *Atmos. Environ.*, *42*(2), 390–402, doi:10.1016/j.atmosenv.2007.09.044.

Durant, A. J., and W. I. Rose (2009), Sedimentological constraints on hydrometeor-enhanced particle deposition: 1992 eruptions of Crater Peak, Alaska, *J. Volcanol. Geotherm. Res.*, *186*(1–2), 40–59, doi:10.1016/j.jvolgeores.2009.02.004.

Eckhardt, S., A. J. Prata, P. Seibert, K. Stebel, and A. Stohl (2008), Estimation of the vertical profile of sulfur dioxide injection into the atmosphere by a volcanic eruption using satellite column measurements and inverse transport modeling, *Atmos. Chem. Phys.*, *8*(14), 3881–3897.

Fioletov, V. E., E. Griffioen, J. B. Kerr, D. I. Wardle, and O. Uchino (1998), Influence of volcanic sulfur dioxide on spectral UV irradiance as measured by Brewer spectrophotometers, *Geophys. Res. Lett.*, *25*(10), 1665–1668, doi:10.1029/98GL51305.

Gerasopoulos, E., P. Zanis, C. Papastefanou, C. S. Zerefos, A. Ioannidou, and H. Wernli (2006), A complex case study of down to the surface intrusions of persistent stratospheric air over the eastern Mediterranean, *Atmos. Environ.*, *40*(22), 4113–4125, doi:10.1016/j.atmosenv.2006.03.022.

Mastin, L., et al. (2009), A multidisciplinary effort to assign realistic source parameters to models of volcanic ash-cloud transport and dispersion during eruptions, *J. Volcanol. Geotherm. Res.*, *186*(1–2), 10–21, doi:10.1016/j.jvolgeores.2009.01.008.

Prata, A. J. (1989a), Infrared radiative transfer calculations for volcanic ash clouds, *Geophys. Res. Lett.*, *16*(11), 1293–1296, doi:10.1029/GL016i011p01293.

Prata, A. J. (1989b), Observations of volcanic ash clouds in the 10–12 μm window using AVHRR/2 data, *Int. J. Remote Sens.*, *10*(4), 751–761, doi:10.1080/01431168908903916.

Servranckx, R., and P. Chen (2004), Modeling volcanic ash transport and dispersion: Expectation and reality, in *Proceedings of the Second International Conference on Volcanic Ash and Aviation Safety*, edited by S. Williamson, pp. 3.1–3.5, U.S. Dep. of Comm., Washington, D. C.

Sparks, R., M. Bursik, S. Carey, J. Gilbert, L. Glaze, H. Sigurdsson, and A. Woods (1997), *Volcanic Plumes*, John Wiley, Hoboken, N. J.

Stocki, T., et al. (2008), Measurement and modelling of radioxenon plumes in the ottawa valley, *J. Environ. Radioactivity*, *99*(11), 1775–1788, doi:10.1016/j.jenvrad.2008.07.009.

Tupper, A., S. Carn, J. Davey, Y. Kamada, R. Potts, F. Prata, and M. Tokuno (2004), An evaluation of volcanic cloud detection techniques during recent significant eruptions in the western "Ring of Fire," *Remote Sens. Environ.*, *91*(1), 27–46, doi:10.1016/j.rse.2004.02.004.

U. S. Geological Survey (1990), The eruption of Redoubt volcano, Alaska, December 14, 1989–August 31, 1990, *Circular 1061*, Denver, Colo.

van Dop, H., et al. (1998), ETEX: A european tracer experiment; observations, dispersion modelling and emergency response, *Atmos. Environ.*, *32*(24), 4089–4094, doi:10.1016/S1352-2310(98)00248-9.

Webley, P., B. Stunder, and K. Dean (2009), Preliminary sensitivity study of eruption source parameters for operational volcanic ash cloud transport and dispersion models – A case study of the August 1992 eruption of the Crater Peak Vent, Mount Spurr, Alaska, *J. Volcanol. Geotherm. Res.*, *186*(1–2), 108–119, doi:10.1016/j.jvolgeores.2009.02.012.

World Meteorological Organization (2007), *Manual on the Global Data-Processing and Forecasting System, Global Aspects*, Geneva.

Wotawa, G., et al. (2003), Atmospheric transport modelling in support of ctbt verification–Overview and basic concepts, *Atmos. Environ.*, *37*(18), 2529–2537, doi:10.1016/S1352-2310(03)00154-7.

D. Bensimon, R. D'Amours, J.-P. Gauthier-Bilodeau, A. Malo, R. Servranckx, and S. Trudel, Canadian Meteorological Centre, 2121 North Service Rd., Trans-Canada Highway, Dorval, QC H9P 1J3, Canada. (real.d'amours@ec.gc.ca)